

Prediction of Heat Transfer Coefficient of Two Phase Flow Sodium Reactor Based on Artificial Neural Network

Yangyang Yang, Zhan Wang*

Collage of Physics and Electronic Engineering, Northwest Normal University, Lanzhou, Gansu 730070, China

* Corresponding author: Zhna Wang (Email: 1003130824@qq.com)

Abstract: Liquid sodium metal is one of the main coolants for fast neutron reaction in nuclear reactors with high heat load and high thermal conductivity. Sodium reactor is one of the most promising and commercialized reactor types in modern nuclear power system. Because the chemical properties of liquid sodium metal are very active, so in a sealed environment, it is easy to react with oxygen, water and other substances, resulting in an explosion. Therefore, it is necessary to design a reasonable experimental circuit and conditions under the appropriate experimental environment to carry out the experiment. With liquid metal sodium as the experimental medium, this paper studies the flow heat transfer characteristics of a two-phase flow sodium reactor by establishing a mathematical model. The key heat transfer parameters in a two-phase flow sodium reactor are predicted by building an artificial neural network model, and the parameters affecting the network performance are adjusted by the artificial neural network. The error of the final result predicted by the adjusted artificial neural network model is within the range of $\pm 10\%$. The prediction results show that the prediction by the artificial neural network model has higher prediction accuracy.

Keywords: Sodium reactor; Flow and heat transfer; Two-phase flow; Mathematical model; Neural network.

1. Introduction

For nuclear reactor, core cooling has always been one of the most important problems in the development of nuclear energy, if the core melting, will bring people incalculable losses. Compared with traditional coolant, liquid sodium metal has the advantages of strong thermal conductivity, high heat load, high thermal inertness, low melting point and high boiling point, which meet the basic conditions of nuclear reactor coolant, and has attracted wide attention from scholars in recent years. Liquid sodium metal can be used to cool the heat generated by fission in nuclear reactors. Compared with other types of reactors, the sodium cold fast reactor with liquid sodium metal as heat carrier has the advantage of long life of nuclear waste, which can make the radioactive waste transmutation and greatly shorten its half-life, which can well solve the problem of nuclear waste disposal. High utilization rate of uranium resources; With better inherent safety performance.

The research on two phase flow in reactor started in 1930. In 1938, Ledinegg [1] studied the correlation characteristic curve of the heating channel under the condition of natural and forced convection, and proposed that the flow drift had variability. In 1949, Lockhart et al. [2] carried out flow experiments of various liquid substances and air doped in horizontal tubes and pointed out the frictional pressure drop gradient relation based on the phase separation flow model. In the 1950s, due to the commercial use of reactors and the development of high parameter boilers, researchers became interested in such two-phase flow topics as critical heat flux (CHF), critical flow, cavitation distribution, and flow instability characteristics. In the 1970s, because of the need of safety analysis, the industry shifted its focus to the complex flow phenomena under the reactor geometry such as blowout and reflooding. The Three Mile Island accident in 1979 made the research focus shift from large rupture accident to small

rupture accident, and natural circulation and reverse flow restriction became important research topics. In the 1990s, how to increase the capability limit of reactor safety analysis procedures became a focus of discussion. System analysis procedures and subchannel analysis procedures were developed from constitutive models and verification experiments. With the rapid development of methods for measuring two-phase flow and the rapid rise of computer and Internet technology, the research on two-phase flow has been progressing since 2000. It supports the research on the basic mechanism of interface evolution of two-phase flow and two-phase propagation under extreme conditions. As the data processing capability of computers continues to improve, more and more researchers use computational fluid dynamics software to explore two-phase flow problems, and build large computing platforms to carry out research on multi-physical intersection problems such as nuclear thermal coupling. Many researchers have studied the two-phase flow problem in fission nuclear energy reactor. Jing Jiangang, Chen Guankuan, Zhou Yunlong et al. [3] established the governing equation of reactor steam generator based on the correlation characteristics of two-phase flow variable density model, in which the system density changes periodically due to the mixing of steam and water states. By using the small disturbance linearization method and the stability criterion of Laplace transform and automatic control theory, the prediction model of specific density wave pattern pulsation was proposed. Yan Xuesong et al. [4] conducted a specific study on the two-phase flow problem of nuclear power system reactors by means of numerical simulation for accelerator-driven two-phase flow reactors. Zhao et al. [5] trained ANN to predict the state of Nusselt number under the transitional boiling condition, and they reached the conclusion based on the experimental data of aggregate boiling on the circular surface downward of a pressure pool with high pressure.

At present, two phase flow reactors such as sodium-cooled

fast reactor and heat pipe reactor use DC steam generator as the key experimental device for heat exchange. The reliability and energy-saving problems of fast reactor power plant are closely related to its thermal and hydraulic characteristics. In the process of reactor operation, the steam generator is prone to mud deposition, fluid-induced vibration, corrosion, wear, fatigue failure and so on, leading to the failure or even rupture of the heat transfer tube. Because the steam generator has a large structure and many loops in the loop, its structure is very fine. Therefore, there are some problems in the experiment, such as high difficulty, long cycle, high cost and huge input of human and material resources, and many key local parameters are difficult to obtain through the experiment. Therefore, this paper will adopt numerical simulation method to study the reactor two-phase flow problem to make up for the shortcomings of the experiment, and use artificial neural network to build the two-phase flow neural network algorithm prediction model.

2. Experimental System

2.1. Composition of sodium-cooled fast reactor system

The sodium-cooled fast reactor usually consists of three heat transfer circuits. The primary system is also called the pool structure, which is distributed with many loops. The primary sodium circulation system is composed of the heat exchanger and the main pump in all loops, including the reactor core in the loop, the connecting pipe, the grid plate coupling box and the sodium pool. In the vapor-water loop, liquid water is heated by heat in the evaporator to form steam. Heat in the evaporator is obtained by the circuit from the heat exchanger and then transferred into it. The liquid sodium in the sodium pool is processed by the sodium pump and transferred to the heat exchanger and the reactor core. See Figure 2.1. The heat exchanger, sodium pump, reactor core and connecting pipeline are distributed in the same sodium pool into a whole, that is, the pool arrangement, the high temperature liquid sodium and low temperature liquid sodium are separated in the sodium pool, sodium circulation pump is mainly used to transfer the low temperature liquid sodium flow to the sodium pool, the low temperature liquid sodium from the sodium circulation pump to the reactor core bottom to be received. Then the low temperature liquid sodium will flow backward through the fuel assembly from bottom to top until its temperature is heated to about 550°C. The high temperature liquid sodium flows from the top of the reactor core through the heat exchanger to the sodium in the loop, so that the temperature drops to about 400°C. Then the high temperature liquid sodium continues to flow to the main and inner shell of the sodium pool, and is finally delivered to the reactor core through the primary route.

The loop distribution of sodium-cooled fast reactor is connected to the sodium pump, reactor and heat exchanger by a pipeline. After a primary circuit, the heat from the reactor core is transferred to the three circuits, thus generating power for the turbo-generator (Figure 2.2).

The steam generator group (generally including evaporator and superheater two areas), the specific schematic diagram is shown in Figure 2.3(a) and (b). According to Figure 2.3(a), the evaporator passes through different sections along the axial direction through the feed water. Each section is controlled by a different control body, and each control body has only one phase state. The heat transfer relationship of different sections

varies according to specific conditions [6]. According to Figure 2.3(b), a large amount of steam will appear in the evaporator through different sections, and the high-temperature steam will pass through the superheated steam area to the superheated area. After the superheater treatment, the high-temperature steam eventually into a single phase form.

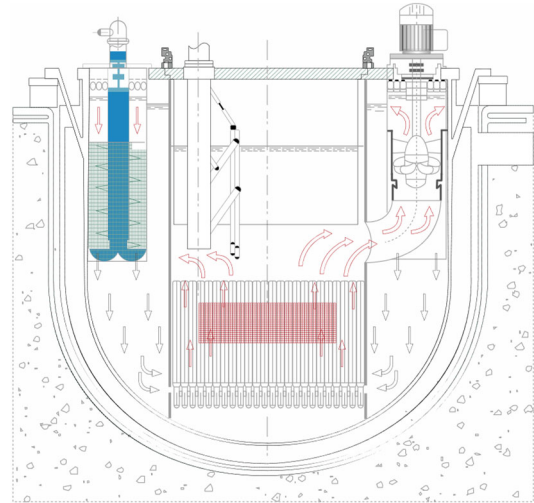


Figure 2.1. Schematic diagram of the pool fast reactor system

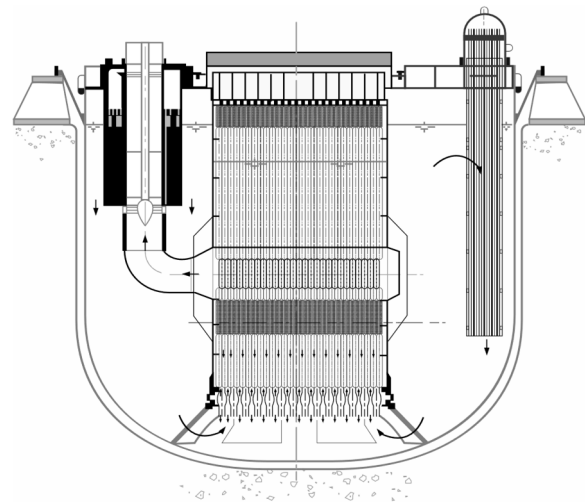


Figure 2.2. Schematic diagram of loop fast reactor system

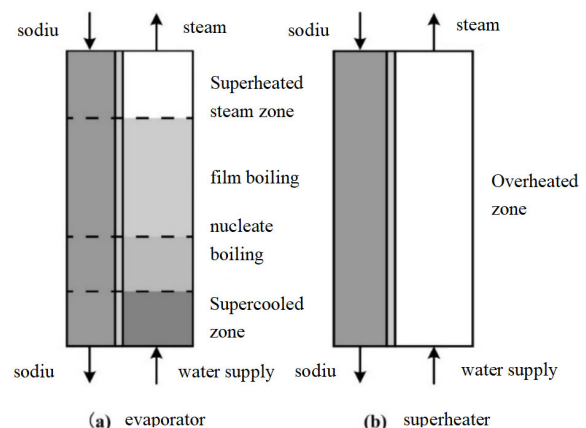


Figure 2.3. Zoning diagram of steam generator

As with the primary, the loops are distributed in the second

loop. Each loop is mainly composed of evaporator group, sodium pump, intermediate heat exchanger and distributor [7]. In the second loop, the reactor unit receives heat from the sodium pump, and this heat is passed from the reactor unit to the evaporator, where a large amount of high-temperature steam is formed. And adjust some related parameters when liquid sodium enters the loop. The steam turbine will process the steam flowing into it. Water-steam circuit is also known as the third circuit, which mainly includes feed pump, evaporator, connecting pipe, etc. [8]. See Figure 2.4 for the specific loop layout of evaporator in sodium-cooled fast reactor. Six steam generator modules are arranged on each side of the three circuit, and three branches are respectively in each loop of the three circuit. The branch is responsible for arranging the regulating valve, which can control the fluid pressure, temperature and flow rate in the branch. When water is supplied from the water supply regulator in the loop, water is distributed to the branch.

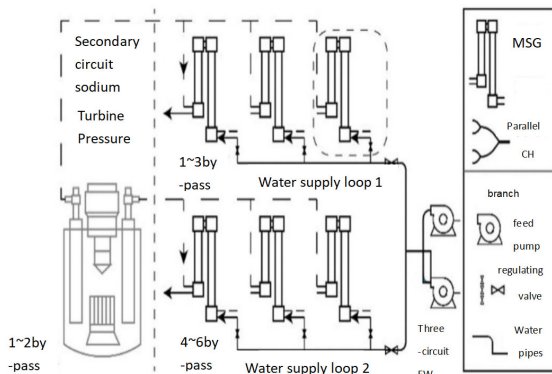


Figure 2.4. Schematic diagram of steam generator layout in sodium-cooled fast reactor

The sodium-cooled fast reactor is located in two loops of the steam generator, as shown in Figure 2.5. The third loop of the steam generator receives the liquid sodium flowing in through the second loop, at which time the steam generator will feed water. Superheater and steam generator serve as inlet and outlet of liquid sodium respectively. The loop transport water to the steam generator as the inlet channel, high temperature steam through the superheater is discharged.

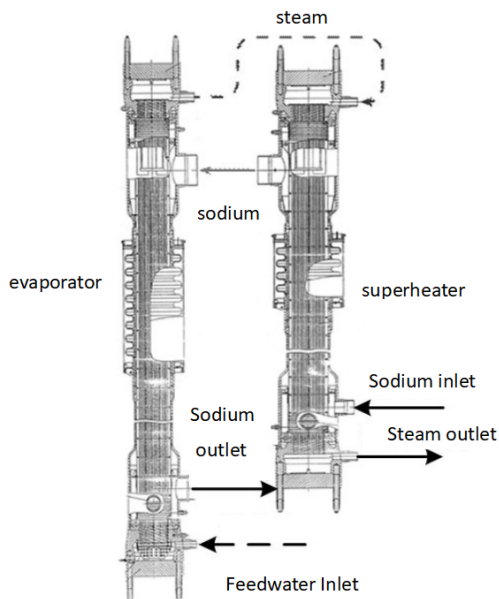


Figure 2.5. Working principle of steam generator

The steam generator operation process is mainly accomplished by heat transfer between the water/steam on the tube side and the liquid sodium on the shell side. When water enters the steam generator, the first thing that occurs is supercooling. The tube side water/steam receives liquid sodium flowing from the shell side as it is heated through the tube wall. The superheater heats the steam as it passes through the membrane and nuclear boiling zones, and the steam that continues to heat up is processed as it passes through the turbine.

2.2. Establishment of mathematical model of evaporator

2.2.1. Basic Assumptions

As the coolant of sodium-cooled fast reactor, all the factors of liquid metal sodium should be taken into account in the practical application process. Therefore, the following assumptions should be put forward when establishing the mathematical model of the sodium-cooled fast reactor water-steam generator:

Evaporator adopts the mode of single tube model;

The heat transfer in the same direction as the central axis and the pipe wall is not considered;

3) The density change of liquid sodium during the flow process will be ignored;

4) The liquid sodium cannot flow backward in the evaporator.

2.2.2. Basic Equation

Based on the assumptions of the steam generator model, the wall of the hot tube and the axial thermal conductivity of the fluid, the following equation is given for the sodium-cooled fast reactor water-steam generator model [7]:

Mass conservation equation:

$$\frac{\partial \rho}{\partial t} = \pm \frac{\partial G}{\partial z} \quad (1)$$

Energy conservation equation:

$$\frac{\partial(\rho H)}{\partial t} = \pm \frac{\partial(GH)}{\partial z} \mp \frac{Q}{A} + \frac{\partial \rho}{\partial t} \quad (2)$$

Momentum conservation equation:

$$\mp \frac{\partial G}{\partial t} = -\frac{\partial}{\partial z} \left(\frac{G^2}{\rho} \right) - \frac{\partial P}{\partial z} - \frac{1}{2} \frac{G^2}{\rho} f_f \frac{U}{A} - \rho g \sin \theta \quad (3)$$

The model equation of two-phase flow homogeneous model is:

$$\rho = (1 - \alpha)\rho_f + \alpha\rho_g \quad (4)$$

$$\rho H = (1 - \alpha)\rho_f H_f + \alpha\rho_g H_g \quad (5)$$

The equations of mass, energy and momentum conservation equation corresponding sodium symbol \pm lateral fluid heat transfer process, while \mp corresponds to the water/steam side. Because water/steam in steam generator in the current state, so the evaporator nuclear θ value is the

opposite of superheater, The former is $\theta = 90^\circ$, while the latter is $\theta = -90^\circ$.

The energy conservation equation in the tube wall is:

$$\pi(r_o^2 - r_i^2)\rho_m C_m \frac{\partial T_m}{\partial t} = q_p - q_s \quad (6)$$

In the above equation, the heat flux is respectively:

$$q_p = 2\pi r_0 h_p (T_p - T_m) \quad (7)$$

$$q_s = 2\pi r_i h_s (T_m - T_s) \quad (8)$$

Where: q_p is the heat flow rate per unit length of fluid received by the sewer side from the wall, the unit is MW/m; q_s is the fluid heat flow received by the wall from the sodium side under the heat flow per unit length, in MW/m. T_m is water wall tube temperature of the surface temperature, unit for $^\circ\text{C}$; The C_m for the heat capacity of the wall, the unit of $\text{J}/(\text{kg} \cdot ^\circ\text{C})$.

Organize the above formula into:

$$(r_o^2 - r_i^2)\rho_m C_m \frac{\partial T_m}{\partial t} = 2r_0 h_p T_p + 2r_i h_s T_s - 2T_m (r_0 h_p + r_i h_s) \quad (9)$$

2.2.3. Sodium side heat transfer model

According to the research on the basic governing equation of the water-steam generator of sodium-cooled fast reactor, the sodium-side convective heat transfer coefficient adopts the Subbotin relation [8]:

$$Nu = 0.58 \left[\frac{2\sqrt{3}}{\pi} \left(\frac{P_t}{D_o} \right)^2 - 1 \right]^{0.55} Pe^{0.45} \quad (10)$$

Where: Nu is Nusselt number; Pe is Bekele number; D_o is the outer diameter of the pipe, m; P_t is the grid distance, m.

2.2.4. Water side heat transfer model

1) Heat transfer model of subcooling zone. The fluid is supercooled water, and the heat transfer mechanism is convective heat transfer of single-phase fluid. The commonly used Dittus-Boelter formula [9] is adopted:

$$Nu = 0.023 Re^{0.8} Pr^{0.4} \quad (11)$$

Where: Nu is Nusselt number; Re is Reynolds number; Pr is the Prandtl number.

Nuclear boiling zone heat transfer model. In the process of natural convection, as the temperature difference between the two phases decreases gradually, the heat increases continuously, resulting in the formation of nuclear boiling. For this phenomenon, a relatively broad THOM[10] formula is adopted:

$$\Delta T_{sat} = 22.53 \left(\frac{q}{10^6} \right)^{0.5} e^{-p/8.69} \quad (12)$$

3) Membrane boiling zone heat transfer model. Miropolskiy[11] formula was adopted for the empirical equation of heat transfer in the boiling region of film state:

$$Nu = 0.021 Re^{0.989} Pr^{0.43} Y_f \quad (13)$$

Among them:

$$Y_f = [1 - 0.1 \left(\frac{\rho_f}{\rho_g} \right)^{0.4} (1-x)^{0.4}] \left[x + \frac{\rho_f}{\rho_g} (1-x) \right]^{0.8} \quad (14)$$

4) Heat transfer model in overheated area. Bishop[12] applied high pressure and high Planck number steam to heat transfer in overheated area as follows:

$$Nu = 0.0073 Re^{0.886} Pr^{0.61} \quad (15)$$

3. Artificial Neural Network Model

Artificial neural network (ANN) is a way processed and realized by computer to imitate the learning behavior of human brain according to its operating mechanism. Artificial neural network abstracts the operation mechanism of the human brain from the objects to be processed into a simple neural network, so as to establish a simple neuron model. The differences between neural networks are mainly classified according to the different ways of contact between neurons by the human brain, and each node in the neural network represents different functions.

3.1. Basis of biology and MP model

By processing a large number of experimental data and samples, ANN provides a complex network model structure to fit the experimental data. Therefore, ANN is often applied to solve arithmetic problems without arithmetic solutions or relatively difficult arithmetic problems. Prediction by using ANN method can be more efficient in terms of data processing accuracy.

Biology is the foundation of ANN, and the two are closely linked. Similar to the biological nervous system, in a biological neural network, neurons are connected to other neurons to establish connections, and the stimulated neurons generate excitement, which transmits a chemical to the connected neurons that changes their electrical potential. If the neuronal potential has exceeded its critical value, the neuron can be "awakened" and transfer chemicals to other neurons. And this model of making connections between neurons by passing certain chemicals is the M-P neuron model. The structure of biological neurons is shown in Figure 3.1.

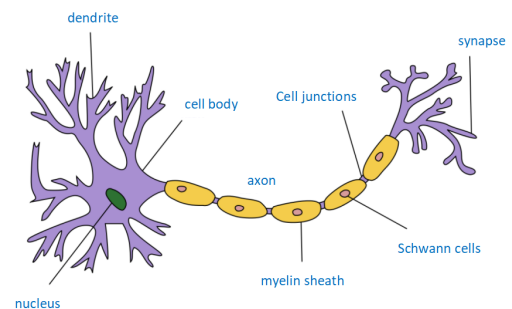


Figure 3.1. Structure of biological neurons

Several important tissues that make up biological neurons are dendrites, axons and cell bodies. The dendrite is the primary tissue of the whole neuronal structure. It is a short, branching tissue extending from the neuronal cell body. It responds to different signals produced by the neuron, and these responses act as input ports for the whole neuron. As the output port, the axon receives different signals from the dendrites after receiving the response. After the signals generated by these neurons reach the axon, the information carried by them will be sent out.

The MP model simulates the external stimulus as a series of digital inputs, simulates the stimulation processing process of each dendrite to the input as a weighted input, simulates the processing of the input by the nucleus as a summation process with bias, and the final output is obtained by nonlinear transformation of the summation result with activation function. Therefore, in the MP model (as shown in Figure 3.2), the corresponding relationship between input and output [13] :

$$y_j = f\left(\sum_{i=1}^m \omega_{ij}x_i + b_k\right) \quad (16)$$

Type of x_i as the input signal, the ω_{ij} for the connection weights, b_k for the positive and negative voltage offsets, $f()$ as the transfer function.

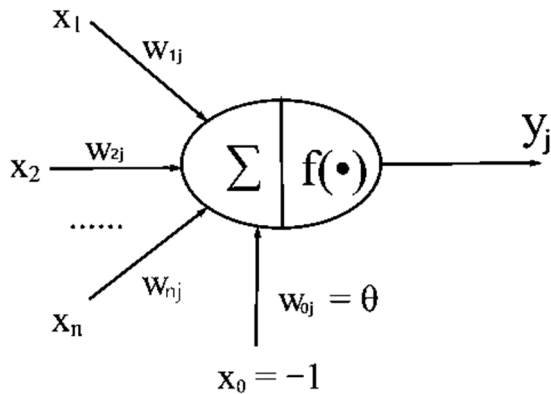


Figure 3.2. MP model

3.2. Overview of BP neural network

BP neural network is a kind of neural network that connects all layers together by weight, and then the input, hidden and output layers are trained according to the reverse algorithm. The specific diagram is shown in Figure 3.3 [14]. The node type considered in this paper is the error back propagation type, that is, the node type of one-way propagation. As a specific type of ANN, BP neural network has generalization ability, nonlinear mapping ability, adaptive ability and self-learning ability, as well as fault tolerance ability. Therefore, BP neural network can be used to predict and analyze the heat transfer coefficient in two-phase flow sodium reactor.

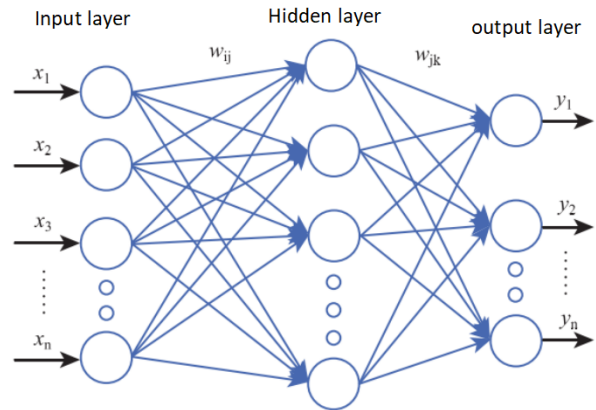


Figure 3.3. Diagram of BP neural network

When propagating BP neural network, it will go through the following two opposite propagation modes according to different situations. The first way is forward propagation. The process of forward propagation is that the input data through the hidden layer and finally transmits it to the output layer depression. The second way is error back propagation. If the output result obtained by the output layer is different from the expected result, the neural network will send the error information of the output result to each layer in reverse, so as to adjust the weight. This is the back propagation. This process is repeated until the error meets the expectation and the prediction is output. As shown in Figure 3.4, the overall work flow of BP neural network is as follows.

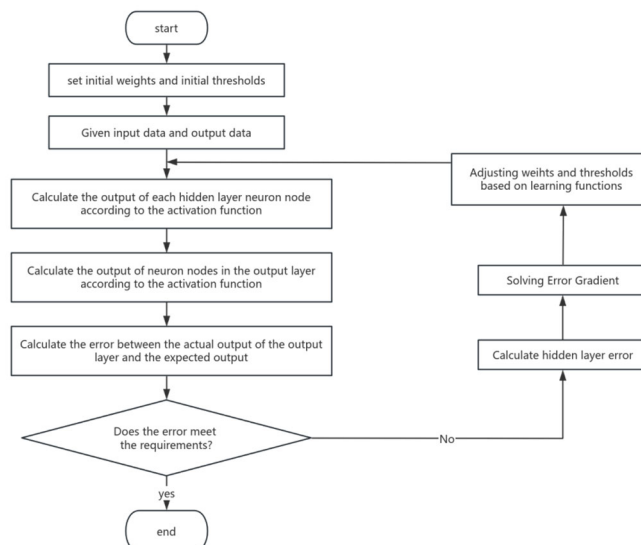


Figure 3.4. BP neural network flow chart

3.3. Model Establishment

An artificial neural network model was constructed to predict the parameters of the mathematical model of two-phase flow sodium reactor evaporator. Re and Pr were taken as input parameters of the neural network, and Nu was taken as output parameters of the neural network. With input parameters as independent variables and output parameters as dependent variables, the input and output of the artificial neural network model can be correlated as follows:

$$Nu = f(\text{Pr}, \text{Re}) \quad (17)$$

The artificial neural network needs to use the normalization method to process the experimental data in order to reduce the influence on the whole network due to the large errors of individual data in the process of data preprocessing. After data normalization adjustment, the training accuracy of the neural network model is obviously improved.

The experimental data can be guaranteed within the range of [0,1] by means of pre-processing.

$$x^* = \frac{x - x_{\min}}{x_{\max} - x_{\min}} \quad (18)$$

Where x^* is the experimental data obtained after normalization processing, x_{\max} is the maximum value and x_{\min} is the minimum value of all experimental data.

After the training of all experimental data is terminated, the artificial neural network reverse-restores all experimental data according to the proportion of normalization, and obtains:

$$x = x^* (x_{\max} - x_{\min}) + x_{\min} \quad (19)$$

Because the artificial neural network takes the mean square error as an important parameter to evaluate the network performance, the artificial neural network often adjusts the weight by gradient descent method. According to the algorithm process of gradient decline to seek the optimal solution, the weights in the output layer and hidden layer can

be adjusted, and the adjusted quantity $w_{ij}(m)$ is as follows:

$$\Delta w_{ij}(m) = -\eta(d_j - y_j(m))f'_2\left(\sum_{i=1}^l w_{ij}(m)a_i^1(m)\right)a_i^1(m) \quad (20)$$

The weight between output layer and hidden layer optimized by gradient descent method is:

$$\Delta w_{ij}(m+1) = w_{ij}(m) + \Delta w_{ij}(m) \quad (21)$$

Adjust the weight between the input layer and the hidden layer, and the adjustment quantity $w_{ij}(m)$ is:

$$\Delta w_{ij}(m) = -\eta(d_j - y_j(m))f'_2\left(\sum_{i=1}^l w_{ij}(m)a_i^1(m)\right)a_i^1(m) \quad (22)$$

The weights obtained after the adjustment of the input layer and the hidden layer are:

$$\Delta w_{ki}(m+1) = w_{ki}(m) + \Delta w_{ki}(m) \quad (23)$$

The selection of hidden layers of artificial neural network will affect its training accuracy. In order to prevent over-fitting of data prediction, the number of hidden layers can be selected by adjusting the range of the given number of neurons by weight [15]:

$$l = a + \sqrt{n + m} \quad (24)$$

Where l is the number of hidden layer neurons; a is a constant, ranging from 1 to 10; m is the number of neurons in the output layer; n is the number of neurons in the input layer.

The number of neurons in the input layer and the number of neurons in the output layer of the artificial neural network are 2 and 1, so the range of hidden layer neurons is [2,12]. While increasing one neuron for training, in order to more accurately set the most appropriate number of neurons for neural network training, the number of neurons in the initial hidden layer is selected from 2 for training until the number of neurons in the hidden layer reaches 12.

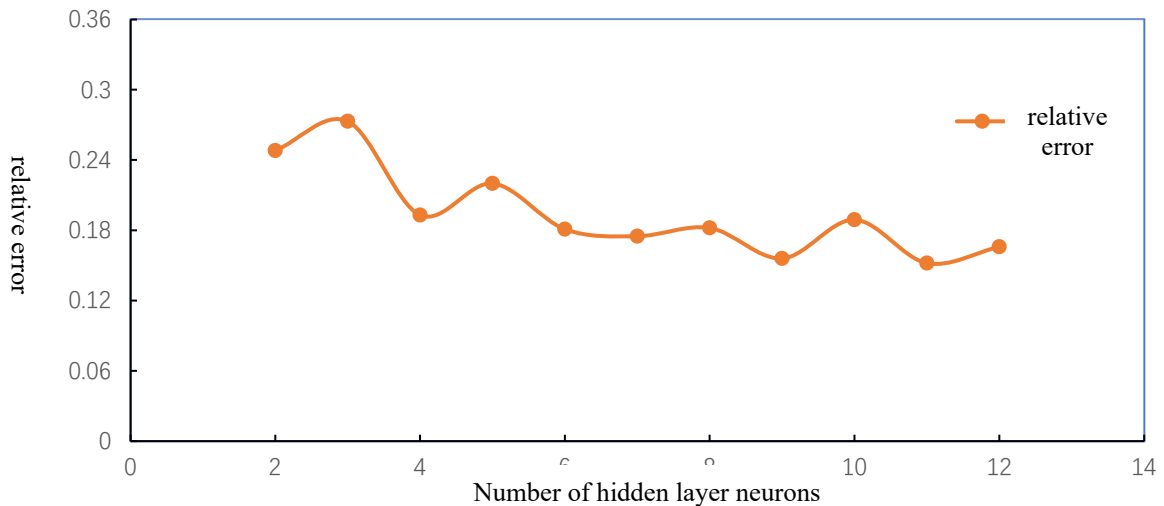


Figure 3.5. Relative error changes with the number of neurons in the hidden layer of ANN

After repeated training for each number of hidden layer neurons, the highest relative error value and the lowest error value which have great influence on the data are removed, and the remaining relative errors are averaged. The results are shown in Figure 3.5. When the number of neurons in the hidden layer is set to 11, the relative error is minimum. Therefore, this paper chooses 11 as the number of hidden layer neurons to be set.

The training objectives, learning efficiency, number of

iterations, training function, transfer function and other parameters of artificial neural network are set as shown in Table 1. The nonlinear Levenberg-Marquardt method combined with gradient descent method is selected for parameter adjustment of the training function, and the training is carried out in MATLAB toolbox. The transfer function selects the nonlinear function tansig for the ANN hidden layer to transmit, and the linear function Purelin for the ANN output layer to transmit.

Table 1. Parameter design of artificial neural network

Training objective	Learning efficiency	Number of iterations	Training function	Transfer function
0.00001	0.1	1000	LM	tansig, purelin

4. Forecast Results and Analysis

In this paper, through random sampling method [16], 200 groups of experimental data were selected and input into the artificial neural network model for prediction according to the parameter range provided by the two-phase flow sodium reactor evaporator model (see Table 2 for details). Among these data, 160 groups of experimental data were the training set, 20 groups of experimental data were the training set, and the remaining 20 groups of experimental data were the verification set.

Table 2. Parameters range

parameter	Minimum value	Maximum value
Re	0.1	776.06
Pr	0.1	250
Nu	1	77

By comparing the data results of expected value and predicted value, it can be found that the variation error of the curve of expected value and predicted value of heat transfer parameters of sodium reactor steam generator is very small and almost in the same trend. Figure 4.1 shows the final prediction result of artificial neural network. The expected value of the artificial neural network test result is indicated by the blue circle. The red star represents the actual predicted value obtained after artificial neural network training, and the blue box represents the error value between the real predicted value and the expected value.

According to the forecast, the error between the expected value and the predicted value ranges from -10 to 10. This error has met the accuracy range required by practical engineering, and can be well applied to the heat transfer model of sodium reactor steam generator [17].

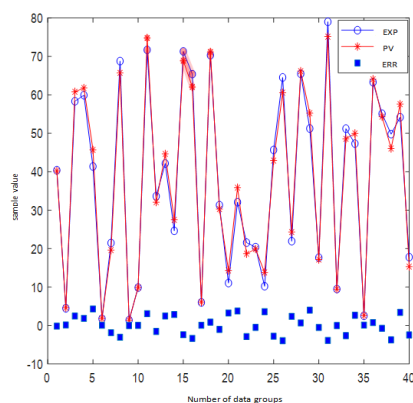


Figure 4.1. Comparison between predicted and actual values of ANN test set

Table 3 lists the actual and predicted values predicted by the artificial neural network model. Through comparative analysis of 40 predicted data points, it is found that more than 95% of the data points have relatively small errors between 0 and 0.2.

Table 3. Actual and predicted values predicted by Ann model

Prediction point	Predicted value	Actual value	Relative error
1	40.21	40.38	0.004
2	4.62	4.47	0.034
3	60.79	58.33	0.042
4	61.76	59.91	0.031
5	45.67	41.37	0.104
6	1.82	1.77	0.028
7	19.61	21.47	0.087
8	65.71	68.77	0.044
9	1.38	1.39	0.007
10	9.90	9.87	0.003
11	74.77	71.69	0.043
12	32.10	33.64	0.046
13	44.63	42.16	0.059
14	27.48	24.63	0.116
15	68.89	71.30	0.034
16	62.04	65.39	0.051
17	6.08	6.01	0.012
18	71.16	70.29	0.012
19	30.29	31.31	0.013
20	14.31	11.05	0.195
21	35.84	32.08	0.117
22	18.67	21.56	0.134
23	19.90	20.39	0.024
24	13.80	10.21	0.352
25	42.89	45.67	0.061
26	60.57	64.52	0.061
27	24.30	21.93	0.108
28	66.15	65.47	0.010
29	55.24	51.24	0.078
30	17.16	17.67	0.029
31	75.12	79.01	0.049
32	9.47	9.48	0.001
33	48.57	51.20	0.051
34	49.97	47.31	0.056
35	2.65	2.54	0.043
36	64.06	63.29	0.012
37	54.33	55.08	0.014
38	46.05	49.78	0.075
39	57.58	54.17	0.063
40	15.32	17.78	0.138

Table 4 once again verifies the accuracy of the above setting results of the ANN hidden layer. When the number of neurons in the hidden layer reaches 11, the ANN training

results are optimal, the relative error is minimum, and the prediction effect is the best. When the number of hidden layer neurons in the artificial neural network model is 11, MAE is 0.311, MSE is 0.156 and RMSE is 0.372.

Table 4. Error results when the hidden layer of Ann model is 11

MAE:	MSE:	RMSE:
0.311	0.156	0.372

Table 5 reflects the reliability of ANN network predictions in different relative error ranges. When the relative error is less than 10%, the reliability of the artificial neural network model is 63.83%. When it is less than 20%, its credibility is 83.61%, when it is less than 30%, its credibility is 90.89% and when it is less than 50%, its credibility is 96.52%. Confidence increases as the relative margin of error increases [18]~[19].

Table 5. Reliability of heat transfer coefficient predicted by Ann model

Relative error	credibility			
	<10%	<20%	<30%	<50%
ANN network	63.83%	83.61%	90.89%	96.52%

The experimental values and predicted values predicted by the artificial neural network model are shown in Figure 4.2. The calculated results well reflect the error between the actual values and predicted values, and the coefficient of determination of the artificial neural network prediction $R=0.99639$. Moreover, the error range between the experimental data and the predicted data points is between -5% and 10%, which verifies that ANN can accurately fit the parameters provided by the sodium reactor evaporator model.

The data in the figure reflect that the experimental value gradually increases with the predicted value obtained by ANN. In this process, the relative error and the absolute error are negatively correlated, with the relative error gradually decreasing while the absolute error gradually increasing.

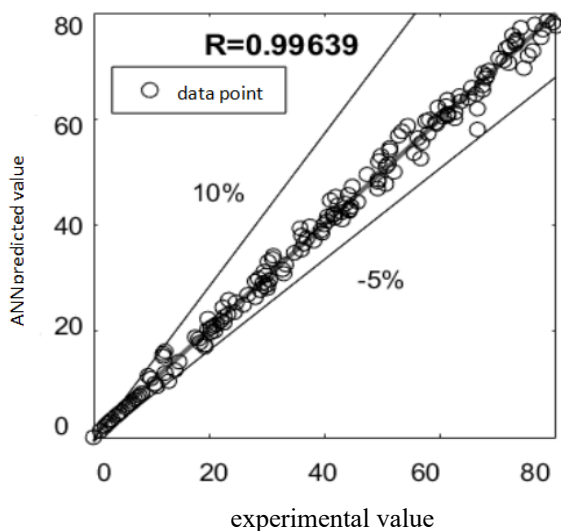


Figure 4.2. ANN calculation results

5. Conclusion

In this paper, the loop and working principle of the sodium-cooled fast reactor system are introduced in detail. The evaporator's multiphase state is divided into four regions: supercooled, nuclear boiling, film boiling and superheated steam. Based on the basic assumption, the equations of each region of the multiphase state are given, and the mathematical model of the water-steam generator of the sodium cold fast reactor is established.

Secondly, the ANN model is established to predict the important parameters in the model, including the normalization of experimental data, and the weight of input layer, output layer and hidden layer is adjusted. By setting the number of neurons in the hidden layer of the neural network, the accuracy of ANN prediction can be effectively improved. After many calculations and the average accuracy is obtained, the number of hidden layers with the best training effect of artificial neural network is 11. By comparing the expected value and predicted value of the experimental data, the error range of the expected value and predicted value is within -10~10. In the artificial neural network, the prediction correlation coefficient $R=0.99639$, indicating that there is a strong positive correlation between the predicted value of the artificial neural network model and the experimental value, with good prediction effect, the mean relative error $MAE=0.061$, the root mean square error $RMSE=0.372$. The error range between data points predicted by ANN model and experimental data is between -5% and 10%. The overall conclusion shows that the artificial neural network can better fit the data, and has a high accuracy, and can be widely used in practical engineering scenes.

References

- [1] LEDINEGG M.I. Stability of flow during natural and forced circulation[J]. Die Wärme, 1938, 48: 61.
- [2] LOCKHART R W, MARTINELLI R C. Proposed correlation of data for isothermal two-phase, two-component flow in pipes[J]. Chem Eng Prog, 1949, 39: 48.
- [3] Jing Jiangang, Chen Xuankuan, Zhou Yunlong. Prediction Model of Two-phase Flow Density Wave Pattern Fluctuation in Integrated reactor Steam Generator [J]. Nuclear Science and Engineering, 1996, (04): 2-9.
- [4] Yan Xuesong, Zhang Xunchao, Zhang Yaling, Yang Yangyang, Gao Xiaofei, Zhang Jianrong, Li Jianyang, Yang Lei, Duan Wenshan. Conceptual study of Accelerator-driven two-phase flow Reactor [A]. Chinese Nuclear Society. Progress Report on Nuclear Science and Technology in China (Vol. 5) -- Proceedings of the 2017 Annual Conference of the Chinese Nuclear Society (Vol. 3) [C]. China Atomic Energy Press: Chinese Nuclear Society, 2017: 5
- [5] D.W. Zhao, G.H. Su, W.X. Tian, K. Sugiyama, S.Z. Qiu. Experimental and theoretical study on transition boiling concerning downward-facing horizontal surface in confined space, Nucl. Eng. Des. 238 (9) (2008) 2460-2467.
- [6] Zhang Xianshan, Sun Peiwei. Research on Feed Water Control Method of Sodium cooled Fast Reactor Multi-module Steam Generator [J]. Automatic Instrumentation, 2019, 40(06): 2530.
- [7] Zhu Lina, Chen Zhenjia, Wu Zhiguang. Analysis of Thermal and Hydraulic Characteristics of Sodium-cooled fast Reactor Steam Generator [A]. Chinese Nuclear Society. Progress Report on Nuclear Science and Technology in China (Vol. 5) - - Proceedings of the 2017 Annual Conference of the Chinese Nuclear Society (Vol. 3) [C]. Chinese Nuclear Society: Chinese Nuclear Society, 2017: 492-497.

- [8] Su Guanghui, Qiu Suizheng, Tian Wenxi, et al. Thermal Hydraulic Calculation Method for Nuclear Power System [M]. Beijing: Tsinghua University Press, 2013:1647.
- [9] Zhang Jianmin, Li Jingguang, Sang Weiliang. Study on Modularization Model and Transient Simulation of Sodium-cooled Fast Reactor Steam Generator [J]. Nuclear power engineering, 1999(1):79-83
- [10] Tzanos C P. A semianalytic method for the solution of the steady-steam generator Equations [J], Nucl. Technol., 1988: 380-391.
- [11] Dittus, F. W., and L. M. K. Boelter 1930, Heat Transfer in Automobile Radiators of the Tubular Type, University of California Publications, vol. 2, pp. 443-461.
- [12] Thom, J. R. S., W. M. Walker, T. A. Fallon, and G. F. S. Reising 1966, Boiling in Subcooled Water during Flow up Heated Tubes or Annuli, Proc. Inst. Mech. Eng. vol. Part 3C, pp. 226-246.
- [13] Miropol'skiy, Z. L. Heat Transfer in Film Boiling of a Steam Water Mixture in Steam Generating Tubes, Teploenergetika vol. 10, pp. 49-53.
- [14] Bishop, A. A., R. O. Sandberg, and L. S. Tong 1965, Forced Convection Heat Transfer at High Pressure after the Critical Heat Flux, American Society of Mechanical Engineering AS-ill-65-HT-31.
- [15] GH Su, K Fukud, DN Jia, et al. Application of an artificial neural network in reactor thermohydraulic problem: Prediction of critical heat flux[J]. Journal of Nuclear Science and Technology, 2002, 39 (5): 564-571.
- [16] Zhang Liming. The Model of Artificial Neural Network and its Application [M]. Shanghai: Fudan University Press, 1993.
- [17] LI Fei. Prediction of heat transfer coefficient of flow boiling by artificial neural network and Genetic Algorithm [D]. Lanzhou University, 2019.
- [18] Ji Nan, Yi Jinhao, Zhao Pengcheng, Yu Tao. Prediction of thermal hydraulic Parameters of Core Based on Adaptive RBF Neural Network [J]. Nuclear Technology, 202, 45(09):69-78. (in Chinese)
- [19] YAN Weiguo, YU Xiaoli, LU Guodong. Thermal Performance analysis of Heat pipe Intercooler based on BP Neural network Method [J]. Journal of Chemical Engineering, 2011, 62(06): 1593-1599.